Application of Multichannel Quantum Defect Theory to the Triatomic van der Waals Predissociation Process

Chun-Woo Lee

Max-Planck-Institut für Strömungsforschung, Bunsenstrasse 10, D-3400 Göttingen, FRG and Department of Chemistry, College of Natural Sciences, Kyungpook National University, Taegu 702-701

Received August 30, 1990

Generalized multichannel quantum defect theory [C. H. Greene *et al. Phys. Rev.*, **A26**, 2441 (1982)] is implemented to the vibrational predissociation of triatomic van der Waals molecules. As this is the first one of such an application, the dependences of the quantum defect parameters on energy and radius are examined carefully. Calculation shows that, in the physically important region, quantum defect parameters remain smoothly varying functions of energy for this system as in atomic applications, thus allowing us very coarse energy mesh calculations for the photodissociation spectra. The choice of adiabatic or diabatic potentials as reference potentials for the calculation of quantum defect parameters as done by Mies and Julienne [*J. Chem. Phys.*, **80**, 2526 (1984)] can not be used for this system. Physically motivated reference potentials that may be generally applicable to all kinds of systems are utilized instead. In principle, implementation can be done to any other predissociation processes with the same method.

Introduction

Since its extensive development by Seaton and his coworkers in the 1950s[1] and reformulation by Fano and his coworkers since 1970,[2,3] the multichannel quantum defect theory (MQDT) is now established in Atomic Physics as one of the most general and powerful theories unifying collision and bound state calculations. It provides a unified treatment of bound and continuum wavefunctions by making use of analytic functions that can be analytically continued from bound to continuum regions or vice versa. It provides also the most general theory of resonance phenomena,[4] describing the complicated resonance structures with a small number of energy insensitive parameters. Accordingly it not only simplifies the task of describing the complicated resonance spectra but also yields great insight into the dynamics of photodissociation or inelastic processes.

However, in spite of its great promise, its application to molecular processes has almost been restricted to the photoionization processes[5] that are dominated by Coulombic interaction and only slightly perturbed by the presence of complicated molecular cores. For the system involving photodissociation processes as parts of the whole process or as a whole process and thus lacking at the long-range interactions such as Coulombic or dipole interaction at the asymptotic region, only a few papers are reported so far by Giusti-Suzor and Jungen,[6] by Mies and Julienne,[7] and by Raoult.[8] Among these, the system treated by Giusti-Suzor and by Jungen and Raoult involves both ionization and dissociation channels. Dissociation processes were not tackled directly simply by ignoring the coupling among dissociation channels. Such a coupling among dissociation channels can not be ignored in the present work and in Mies and Julienne's one because of the absence of the ionization channels. Actually, its treatment is the central theme in the latter. In contrast to the work by Giusti-Suzor and by Jungen and Raoult, *a priori* separate treatment of the reaction and free zone and the analytical treatment for the free zone can not be employed in the present and in the Mies and Julienne's work. Numerical methods should be employed in the large R region. As a consequence of this, the same close coupling equation should be used for all the dissociation space, regardless of whether we are in reaction or free zone (actually, this does not cause much trouble as in the Coulombic case where the numerical treatment of the free zone is notoriously difficult because of the long-range nature of the potential). It could be anticipated that the use of the same equation for both reaction and free zones may make it difficult to satisfy the usual MQDT assumptions and pose a stringent test to MQDT.

Here we report MQDT calculation using the generalized MQDT method proposed by Greene, Rau, and Fano[11] except that a close-coupling algorithm is used at short distances in place of the R-matrix procedure. Their generalized MQDT method adopting Milne's procedure for the calculation of quantum defect parameters is easier to implement than the one by Mies and Julienne. The calculation of close-coupling equations at shorter distances needs only a conventional computer code such as De Vogelaere algorithm (this aspect is not much emphasized in Mies and Julienne's work). Adiabatic or diabatic reference potentials employed in Mies and Julienne's work can not be used for certain channels which are required for the system of interest here in order to get the convergence in the calculation of the S matrix or other observables. Physically motivated reference potentials are used instead, still preserving the convenience. Though such an implementation is here limited to predissociation processes of triatomic van der Waals molecules, there may not be much difficulty in applying the same method to other systems.

The present work deals with the rovibrational predissociation of triatomic molecules, deviating from Mies and Julienne's one which treats the predissociation of diatomic molecules. As a model system, a van der Waals molecule is chosen because of its weak atom-diatomic interaction potential. Because of its weak atom-diatomic interaction potential, the computational time is shorter for it than for other triatomic molecules. It is also a system for which true state-to-state

measurements[9] of intramolecular energy redistribution are available. As this is the first of MQDT application to predissociation processes, basic assumptions of MQDT, such as the slow dependence of the quantum defect parameters on energy and radius, are examined carefully. The comparison of the eigenphase sums obtained from MQDT with the ones from the close-coupling method is made as functions of channel numbers and matching radius. However, application of this analysis to the understanding of the final state population distribution of the diatomic photofragment is deferred as future work. Infinite order sudden approximation[10] (IOS) holds rather well for this system as well. It may be an interesting problem to see IOS from the viewpoint of MQDT. Its physical origin obtained by examing the short-range wavefunctions will be published elsewhere.

In Section II, a summary of MQDT is given. Section IIIA describes the system used in this paper. Calculational procedures are given in Section IIIB. The results and discussions are given in Section IV.

MQDT

In MQDT, the coordinate R along which fragmentation takes place is divided into two ranges $R \leq R_0$ and $R > R_0$. The matching radius R_0 is usually taken so that all inelastic processes are included in the inner space. By taking R_0 in this way, motions of particles in the outer region, and thus observables, are affected by the complicated dynamics occurring in the inner region only through the values of log-derivatives of inner wave functions at the boundary. In the outer space, motions in the different channels are decoupled. The radial wavefunction $F_i(R)$ for the i^{th} channel state Φ_i obeys the ordinary second order differential equation and is generally obtained as a linear combination of regular and irregular solutions $f_i(R)$ and $g_i(R)$. In MQDT, it is customary to consider the standing wave channel basis functions Ψ_i.

$$\Psi_i(R, \omega) = \sum_i \Phi_i(\omega)[f_i(R)\delta_{ii'} - g_i(R)K_{ii'}], \quad R \geq R_0 \tag{1}$$

where ω denotes collectively all the coordinates but R and $K_{ii'}$ is the real symmetric matrix. Note here that the summation index i in (1) runs over channels included in the calculations, not over open channels alone. The classification of closed or open channels can be made only when the boundary conditions are imposed at $R \to \infty$ and is deferred to the final stage in MQDT. Strong energy dependence of observables shows up around resonance and the existence of resonance indicates the presence of a closed channel. The K matrix defined in (1) is thus expected not to show strong energy dependence in general as boundary conditions at $R \to \infty$ are not imposed yet. In other words, the K matrix in (1) is obtained by solving close-coupling equations from origin upto $R = R_0$.

The regular and irregular solutions $f_i(R)$ and $g_i(R)$ normalized per unit energy range have the asymptotic forms for the open channels

$$f_i(R) \to \sqrt{\frac{2m}{\pi k_i}} \sin(k_i R + \eta_i)$$

$$g_i(R) \to -\sqrt{\frac{2m}{\pi k_i}} \cos(k_i R + \eta_i) \tag{2}$$

that clearly exhibit a singularity (branch point) at the threshold owing to the factor $1/\sqrt{k_i}$. Thus we can not analytically continue $f_i(R)$ and $g_i(R)$ across the threshold into the negative energies. Construction of an analytical[12] regular and irregular base pair $f_i^0(R)$ and $g_i^0(R)$ for the predissociation system is thus the starting point for any MQDT analysis, as it leads to a unified treatment of bound and continuum regions and constitues the core of the generalized MQDT of Ref. 11 and Ref. 7. Both base pairs have their own advantages. Energy-normalized base pair is more convenient in treating the dynamics at the asymptotic region while analytical one is more convenient around the threshold region. For the system of interest here where only a finite number of discrete levels can be supported by any particular closed channel, threshold regions may be no longer important as for the Coulombic system. Thus the energy-normalized base pair is employed here for the convenience (even, for the Coulombic system, $f_i(R)$ and $g_i(R)$ do not cause the singularities at the range of energies very close to threshold[13]).

The *energy normalized* $f_i(R)$ and $g_i(R)$ with negative kinetic energies at large R have the asymptotic form[14]

$$f_i(R) \to \sqrt{\frac{m}{\pi\kappa_i}} (\sin\beta_i D_i^{-1} e^{\kappa_i R} - \cos\beta_i D_i e^{-\kappa_i R})$$

$$g_i(R) \to -\sqrt{\frac{m}{\pi\kappa_i}} (\cos\beta_i D_i^{-1} e^{\kappa_i R} + \sin\beta_i D_i e^{-\kappa_i R}) \tag{3}$$

where D plays the role of making $e^{\pm\kappa R}$ terms having the comparable magnitudes at large R, and β_i stands for the accumulated phases.

MQDT now considers "short range" channel basis functions (will be labeled by α) Ψ_α as eigenfunctions of the real symmetric matrix K. The eigenvalues of the K matrix are conveniently parameterized as $\tan \pi\mu_\alpha$ where μ_α (or $\pi\mu_\alpha$) are called eigenquantum defects (eigenphaseshifts). If we denote the collection of eigenvectors of K as the U matrix, then

$$K_{ii'} = \sum_\alpha U_{i\alpha} \tan\pi\mu_\alpha U^\dagger_{\alpha i'} \tag{4}$$

U is thus the transformation matrix (or sometimes called a frame transformation matrix) between the two basis functions. The short-range wavefunctions are then given by

$$\Psi_\alpha = \sum_i \Phi_i(\omega) U_{i\alpha} [f_i(R) \cos\pi\mu_\alpha - g_i(R)\sin\pi\mu_\alpha] \tag{5}$$

and their relation with Ψ_i is obtained as

$$\Psi_\alpha = \sum_i \Psi_i U_{i\alpha} \cos\pi\mu_\alpha \tag{6}$$

The parameters η_i, D_i, β_i, μ_α and $U_{i\alpha}$ in Eqs. (2), (3), and (4) are the whole set of parameters needed in the multichannel quantum defect theory in order to describe the observables such as inelastic cross sections [one more parameter, the transition dipole matrix element $\vec{D}_\alpha = \langle \Psi_{g''} \| \vec{\mu} \| \Psi_\alpha \rangle$, is needed in case of photodissociation cross sections]. In the semiempirical application of MQDT, short-range parameters μ_α and the frame transformation matrix $U_{i\alpha}$ are usually assumed to be constant functions of energy. The energy dependences of the remaining parameters η_i and β_i are known analytically for Coulombic and dipole (attractive) fields but should be calculated numerically in the absence of long-range fields as in the present case.

MQDT now considers energy normalized basis functions Ψ_ρ that satisify the boundary conditions, *i.e.*, that coefficients of the exponentially rising terms are zero at $R\to\infty$ and that all open channels have an identical phase τ_ρ as Ψ_α do (the condition to be eigenchannels). Let Ψ_ρ be given as a superposition of Ψ_α:

$$\Psi_\rho=\sum_\alpha \Psi_\alpha A_{\alpha\rho} \tag{7}$$

Substituting Eqs. (3) and (5) into (7) and applying the boundary conditions, we have

$$\sum_\alpha U_{i\alpha}\sin(\beta_i+\pi\mu_\alpha)=0,\ i\in \text{closed channels}$$

$$\sum_\alpha U_{i\alpha}\cos(\pi\mu_\alpha)A_{\alpha\rho}=T_{i\rho}\cos(\pi\tau_\rho)$$

$$\sum_\alpha U_{i\alpha}\sin(\pi\mu_\alpha)A_{\alpha\rho}=T_{i\rho}\sin(\pi\tau_\rho),\ i\in \text{open channels} \tag{8}$$

$T_{i\rho}$ and τ_ρ replace $U_{i\alpha}$ and μ_α in Eq. (5) with i now running over only open channels at the asymptotic region. The coefficients $A_{\alpha\rho}$ and τ_ρ can be obtained by solving the generalized eigenvalue equation:

$$\Gamma A=\tan\pi\tau\ \Lambda A \tag{9}$$

with their matrix elements given by

$$\Gamma_{i\alpha}=\begin{cases} U_{i\alpha}\sin(\beta_i+\pi\mu_\alpha), & i\in \text{closed channels}\\ U_{i\alpha}\sin(\pi\mu_\alpha), & i\in \text{open channels}\end{cases} \tag{10}$$

$$\Lambda_{i\alpha}=\begin{cases} 0, & i\in \text{closed channels}\\ U_{i\alpha}\cos(\pi\mu_\alpha), & i\in \text{open channels}\end{cases} \tag{11}$$

The relation between the real symmetric $K_{ii'}$ matrix in (1) and the usual reactance matrix K defined at the asymptotic region as following:

$$\Psi_{i'}\to\sum_i \Phi_i(\omega)[f_i(R)\delta_{ii'}-g_i(R)\mathrm{K}_{ii'}],\ \text{when } R\to\infty \tag{12}$$

is given by

$$\mathrm{K}=K^{oo}-K^{oc}[\tan\beta+K^{cc}]^{-1}K^{co} \tag{13}$$

where K^{oo}, $K^{oc}\cdots$, denote the open-open, open-closed... component of the K matrix. The eigenvalues and eigenvectors of K are just tan $\pi\tau_\rho$ and Ψ_ρ considered in (8).

Now wavefunctions satisfying the appropriate boundary conditions can be obtained as a superposition of Ψ_ρ. For example, $\Psi^{-(i)}$ satisfying the incoming wave boundary conditions are given as

$$\Psi^{-(i)}=\sum_\rho C_\rho^{-(i)}\Psi_\rho \tag{14}$$

with

$$C_\rho^{-(i)}=i(T^{-1})_{i\alpha}e^{-i(\sigma_\alpha+\pi\tau_\rho)} \tag{15}$$

Calculational Procedures

System

Empirical potentials for several van der Waals systems, like rare gas-halogen ones such as $NeCl_2$, $HeCl_2$ or interhalogen van der Waals molecules,[15] are well established owing to the state-to-state measurements available for them. The interaction potential between A and B_2 in the AB_2 triatomic system used by Halberstadt *et al.*[16] for $NeCl_2$ has the following form (a slightly modified form for $HeCl_2$)

$$V(R,r,\gamma)=V_M(R,r,\gamma),\ \text{when } R\le R^*,$$

$$V(R,r,\gamma)=V_{vdW}(R,\gamma)+(V_M-V_{vdW})e^{-\beta(R-R^*)^2},$$

$$\text{when } R\ge R^* \tag{16}$$

The Jacobi coordinates R, r, γ in (16) denote the distance between A and the center of mass of B_2, the bond distance of B_2, and the angle between $\vec{R}$ and $\vec{r}$ respectively. $V_M(R,r,\gamma)$ and V_{vdW} are given as

$$V_M(R,r,\gamma)=D_{AB}\sum_i\{\{\exp[-\alpha_{AB}(R_{AB_i}-R_{AB}^{(e)})]-1\}^2-1\}$$

$$+D_{CM}\{\{\exp[-\alpha_{CM}(R_{CM_i}-R_{CM}^{(e)})]-1\}^2-1\} \tag{17}$$

$$V_{vdW}(R,\gamma)=-\frac{C_6(\gamma)}{R^6}-\frac{C_8(\gamma)}{R^8} \tag{18}$$

where R_{AB_i} is the distance between A and i^{th} B atom, R is the same as above. Other parameters are constant and are adjusted to the best fit to the experimental values. Two Legendre terms are retained for $C_6(\gamma)$ and $C_8(\gamma)$, *e.g.*,

$$C_6(\gamma)=C_{60}+C_{62}P_2(\cos\gamma) \tag{19}$$

R^* is chosen in Ref. 16 as the inflection point of the atom-atom Morse potentials and is given by $R^*=R_{CM}^{(e)}+\ln(2/\alpha_{CM})$. The values of parameters used in this paper are slightly different from those of Ref. 16 and are given in Table 1.

Table 1. Values of Potential Parameters Used in This Paper

(a) Morse potential parameters	
$D_{AB}=0.0034$ eV,	$D_{CM}=0.00195$ eV
$\alpha_{AB}=1.0$ a.u.$^{-1}$,	$\alpha_{CM}=1.0$ a.u.$^{-1}$
$R_{AB}^{(e)}=6.82$ a.u.,	$R_{CM}^{(e)}=6.65$ eV
(b) van der Waals potential parameters	
	$C_{60}=0.750$ eV(a.u.)$^{-6}$
	$C_{62}=0.119$ eV(a.u.)$^{-6}$
	$C_{80}=1.580$ eV(a.u.)$^{-6}$
	$C_{82}=0.800$ eV(a.u.)$^{-6}$

With this interaction potential, the Hamiltonian for the triatomic van der Waals molecules AB_2 is given by[17]

$$H=-\frac{1}{2m}\frac{\partial^2}{\partial R^2}+\frac{\vec{j}^2}{2\mu r^2}+\frac{\vec{l}^2}{2mR^2}+V(R,r,\gamma)+H_{B_2}(r) \tag{20}$$

with

$$H_{B_2}(r)=-\frac{1}{2\mu r^2}\frac{\partial^2}{\partial r^2}+V_{B_2}(r) \tag{21}$$

$H_{B_2}(r)$ denotes the vibrational Hamiltonian of B_2. In Eq. (20) and (21), m denotes the reduced mass of A and the center of mass of B_2; μ, the reduced mass of B_2; $\vec{j}$, the angular momentum operator of B_2; and $\vec{l}$, the orbital angular momentum operator of the relative motion of A and the center of mass of B_2.

It is known both experimentally and theoretically that the magnitudes of total angular momentum operator, $\vec{J}=\vec{j}+\vec{l}$, do not affect the predissociation dynamics much. They will be set to zero hereafter. This simplifies the Hamiltonian as $\vec{l}$ can be set to $\vec{j}$. When the wavefunctions $\Psi(R, r, \gamma)$ are expanded in the rovibrational channel basis functions $\Phi_{vj}(r, \gamma)=(r \mid v)\ Y_{j0}(\gamma, 0)$ as

$$\Psi(R, r, \gamma)=\sum_{vj}\chi_{vj}(R)\Phi_{vj}(r, \gamma) \tag{22}$$

the close-coupling equations are given as

$$\left[-\frac{d^2}{dR^2}-k_{vj}^2+\frac{j(j+1)}{R^2}\right]\chi_{vj}(R)$$
$$+2m\sum_{v'j'}V_{vj,v'j'}(R)\chi_{v'j'}(R)=0 \tag{23}$$

with

$$k_{vj}^2=2m[E-Bj(j+1)-(v+\frac{1}{2})\omega] \tag{24}$$

and

$$V_{vj,v'j'}(R)=\int d\gamma \sin\gamma \int dr \Phi_{vj}(r, \gamma)V(R, r, \gamma)\Phi_{v'j'}(r, \gamma) \tag{25}$$

In the practical calculations of $V_{vj,v'j'}(R)$, the interaction potential is expanded into Legendre polynomials and the angle integration is performed analytically to yield the formula in terms of $3j$ symbols.

Computational Aspects of MQDT

Milne procedure. The real symmetric K matrix in (1) is easily obtained by simply replacing $\exp(\pm ik_iR)$ or $\sin k_iR$ and $\cos k_iR$ appearing in the boundary conditions at the matching radius with the energy normalized base pair $f_i(R)$ and $g_i(R)$. The matching radius is taken to lie much insider than the asymptotic region. The subindex i for the coupled equation should now include both open and closed channels in contrast to the usual close-coupled calculation where only open channels are included.

The base pair $f_i(R)$ and $g_i(R)$ satisfies the ordinary second order differential equation and thus may not be difficult to obtain. However, the MQDT requirement to have both regular and irregular pair at the negative energies may cause trouble. As the base pair is singular at $R\rightarrow\infty$ and irregular wavefunctions are singular at the origin, boundary conditions can not be applied to the base pair numerically at both origin and $R\rightarrow\infty$. Though conventional stable computer algorithms[18] that could overcome this difficulty exist, Milne method[19] recommended in Ref. 11 is easy to use and very stable in comparison to the conventional algorithms. Milne method is quite stable even in the deep classically forbidden region and also stable to the step size. This stability derives from the fact that it calculates the more slowly varying functions of radii, *i.e.*, amplitudes and phases of the regular and irregular functions, than the wavefunctions themselves. Besides this advantage, Milne method allows more flexibility in choosing the boundary condition.

In the Milne procedure, the base pair is replaced with $\alpha_i(R)$ and $\phi_i(R)$ by the transformation

$$f_i(R)=\sqrt{\frac{2}{\pi}}\alpha_i(R)\sin\phi_i(R)$$

$$g_i(R)=-\sqrt{\frac{2}{\pi}}\alpha_i(R)\cos\phi_i(R) \tag{26}$$

for both positive and negative energies with $\phi_i(R)$ given in terms of α_i by

$$\phi_i(R)=\int_0^R \alpha_i^{-2}(R')dR' \tag{27}$$

By taking the lower integration limit to be zero, $f_i(R)$ and $g_i(R)$ are insured to be regular and irregular solutions at the origin. The function α_i itself satisfies the ordinary second order differential equation

$$\frac{d^2\alpha_i(R)}{dR^2}+k_i^2(R)\alpha_i(R)=\alpha_i^{-3}(R)$$
$$k_i^2(R)=2m[E-V_{ref}(R)] \tag{28}$$

The term $V_{ref}(R)$, called reference potential, will be discussed in the next subsection. The factor $(2/\pi)^{1/2}$ in Eq. (26) ensures that the base pair has the value of Wronskian, $2/\pi$, just as the energy normalized base pair should do. The boundary conditions for $\alpha_i(R)$ are such that $\alpha_i(R)$ be a slowly varying function of R as far as possible. At the positive energies, such boundary conditions are obtained as

$$\alpha_i(R)\rightarrow k_i^{-1/2},\ \frac{d\alpha_i(R)}{dR}\rightarrow\frac{d}{dR}k_i(R)^{-1/2}=0,\ \text{at}\ R\rightarrow\infty \tag{29}$$

The same conditions as (29) might be obtained if $\alpha_i(R)$ and $\phi_i(R)$ were the amplitude and phase of the WKB wavefunction. At the negative energies, the boundary conditions (29) can not be applied. Applying the same kind of boundary conditions at the potential minimum instead of at the asymptotic region, namely

$$\alpha_i(R_c)\rightarrow k_i^{-1/2}(R_c),\ \frac{d\alpha_i(R)}{dR}\rightarrow\frac{d}{dR}k_i(R_c)^{-1/2}=0 \tag{30}$$

has proposed as a means of reducing the oscillations in $\alpha_i(R)$ and $\phi_i(R)$ as far as possible. (Oscillation problem may be severe for some systems as found in Ref. 20. In the present system, such a problem does not take place.) The quantum defect parameter β_i is identified in the Milne procedure as

$$\beta_i\cong\int_0^\infty \alpha_i(R)^{-2}dR \tag{31}$$

The second order differential equation (28) and the close-coupling equation (23) are solved by the De Vogelaere algorithm[21] which is particularly suitable for the integration of (31) by a Simpson formula since it generates $\alpha_i(R)$ not only at the propagation mesh points but also at their middle points.

So far we described that real symmetric K matrices can be obtained from the usual close-coupling computer code by replacing $\exp(\pm ik_iR)$ with the base pair $f_i(R)$ and $g_i(R)$ and allowing i to belong to closed as well as open channels. This base pair, in turn, is easily obtained by the Milne procedure. The potential needed in this procedure is discussed in the next subsection.

Reference potentials. In case of the Coulombic system, a potential for the calculation of $f_i(R)$ and $g_i(R)$ is conveniently chosen as $-Z/R$. However in the strict sense the potential for the calculation of $f_i(R)$ and $g_i(R)$ can only be

defined unambiguously in the interval, $R \geq R_0$. Or, putting it in another way, the choice of the potential at $R < R_0$ is at our disposal and does not affect the result of MQDT calculation.

The different choice of potentials is utilized first by Dubau and Seaton[22] and its significance is emphasized by Giusti-Suzor and Fano.[23] It is also treated in Ref. 24 in the title of optical potentials. It not only changes the values of long-range quantum defect theory (qdt) parameters but also those of K matrix elements. The transformation formulas between K matrices corresponding to two different reference potentials are given by

$$K = (\sin\pi\mu + \cos\pi\mu\ K')(\cos\pi\mu - \sin\pi\mu\ K')^{-1} \quad (32)$$

where $\sin\pi\mu$ and $\cos\pi\mu$ are diagonal matrices *e.g.*, $\sin\pi\mu_{ij} = \sin\pi\mu_i\,\delta_{ij}$ and $\pi\mu_i$ denotes the phase shifts caused by the difference of the reference potentials.

In the system of our interest, this aspect enters into our consideration from the beginning since the potentials in this case in $R \geq R_0$ are given numerically and one extrapolation to the region of $R < R_0$ does not excel the other extrapolation differing from the Coulombic system.

Two extrapolations using adiabatic and diabatic potentials may be well defined and can be utilized for any system without arbitrariness. Diabatic and adiabatic potentials connected to $\{vj\}$ fragmentation channels are defined as

$$V^{vj}_{diab}(R) = V_{vj,vj}(R) + \frac{j(j+1)}{2mR^2} + Bj(j+1) + (v+\frac{1}{2})\omega \quad (33)$$

and

$$V^{vj}_{adia}(R) = v_{vj}(R) + \frac{j(j+1)}{2mR^2} + Bj(j+1) + (v+\frac{1}{2})\omega \quad (34)$$

where $v_{vj}(R)$ are the eigenvalues of the hermitian matrix $V_{vj,v'j'}(R)$. However, for the system of our interest, these extrapolations can not be applied since the reference potentials from these extrapolations may have potential minima higher than the predissociation resonance energies (see Figure 1 where adiabatic or diabatic potentials connected to $v=1$ and $j=4$ and to $v=1$ and $j=6$ fragmentation channels have potential minima higher than the resonance energy $\simeq$0.0132 eV). Note that particles with negative kinetic energy in all space can not exist. Adding additional diagonal elements of kinetic operator to the reference potentials only makes the potential minima higher [see Eq. (6. 15b) of Ref. 17].

One easy remedy to these potentials is to take the following potential:

$$V_{IOS}(R) = V(R, r_e, \gamma_e) + \frac{j(j+1)}{2mR^2} + Bj(j+1) + (v+\frac{1}{2})\omega \quad (35)$$

as a reference potential in the region of R smaller than some radius R^* and connect this to the adiabatic or diabatic potentials at R^*. (R_e, r_e and γ_e denote the values of R, r and γ at the equilibrium configuration of the van der Waals complex). The connection *e.g.* with diabatic potentials $V^{vj}_{diab}(R)$ corresponding to the $\{v, j\}$ fragmentation channel is made as

$$V_{vj}(R) = \begin{cases} V_{IOS}(R), & R \leq R^* \\ V^{vj}_{diab}(R) + (V_{IOS} - V^{vj}_{diab})e^{-\rho[(R-R^*)/R^*]}, & R \geq R^* \end{cases} \quad (36)$$

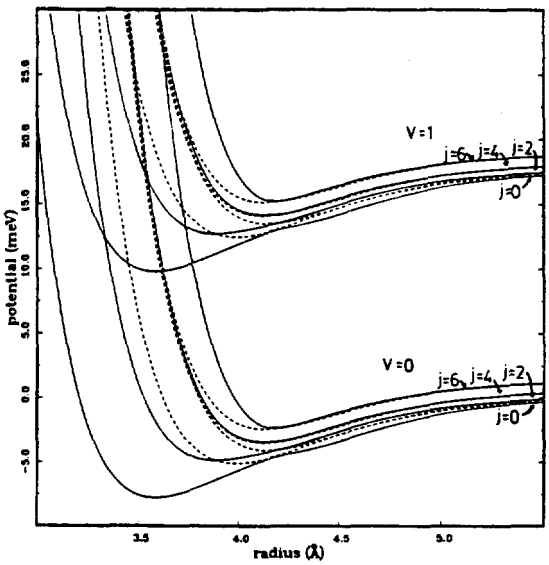

Figure 1. Adiabatic and diabatic potentials calculated with 8 channels for the triatomic van der Waals system with potential parameters given in Table 1. Solid and dashed lines denote adiabatic and diabatic potentials respectively. Their vibrotational quantum numbers v and j are shown in the Figure.

with suitably chosen constants R^* and ρ. [If we consider the energy range below the minimum of V_{IOS} of (36), $V_{IOS}(R)$ with v-1 instead of v may be chosen.]

Other aspects of calculation. In the previous subsections, we described how to obtain a short-range K matrix and long-range quantum defect parameters β_i and η_i. Once the K matrix is given, the frame transformation matrix $U_{i\alpha}$ and eigenquantum defects μ_α can be obtained easily by diagonalizing the K matrix. This calculation requires almost same computational time as that of the close coupling one. We repeat this calculation for coarse energy mesh points. As quantum defect parameters β_i and η_i and short range parameters μ_α and frame transformation matrices are expected to be slowly varying functions of energy, their values at energies off the mesh points can be obtained quite accurately by interpolation. Here, interpolation is performed by a cubic spline fit at each energy mesh point. A computer code for the cubic spline fit may be obtained in the standard math-libraries like IMSL, NAG, Numerical Recipes. With this interpolation, we can solve the generalized eigenvalue equation (9) at any energies. The computational time for the interpolation and the generalized eigenvalue problem can be neglected in comparison with that of the close coupling calculation. Thus by this MQDT calculation with the coarse energy mesh points we can save a lot of computational time.

Results and Discussion

As we said earlier in Section II, in the Coulombic system, most of inelastic processes take place in a very small region of space. In that region, potential energies for the relative motion of particles are so big that the magnitudes of kinetic energies do not vary much as functions of energy of the system. Elastic processes occurring in the region outside R_0 are dominated by the long-range Coulombic potential and

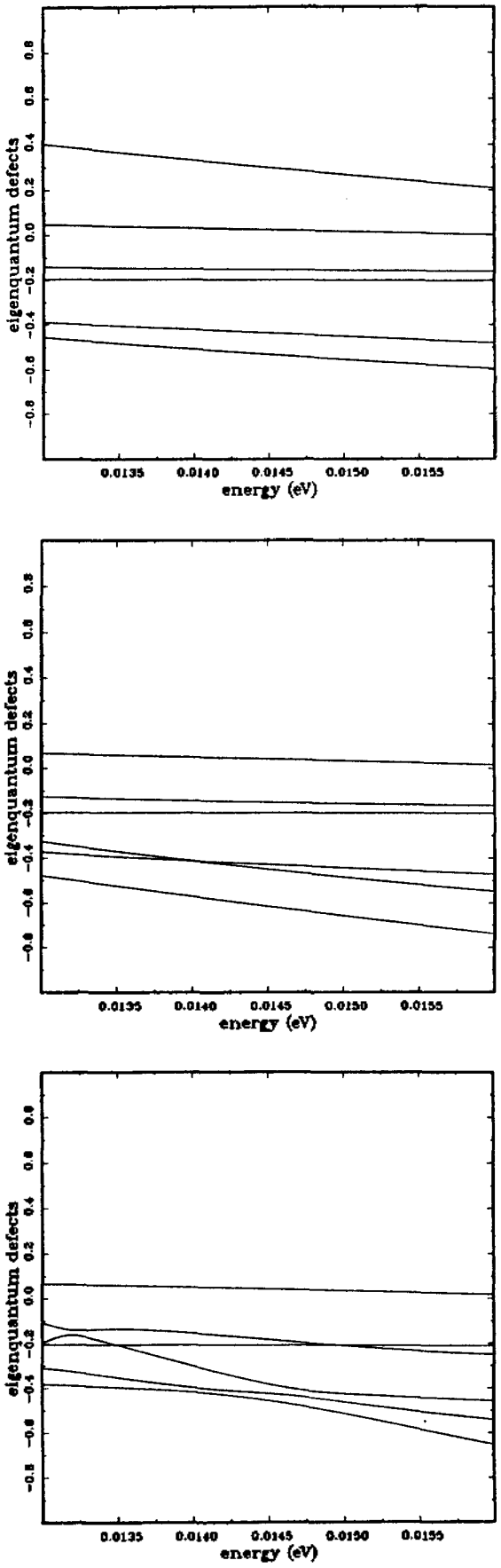

Figure 2. Short-range eigenquantum defects *vs* energy in the 6 channel calculation: (a) for $R_0=4$ Å; (b) $R_0=4.5$ Å; (c) $R_0=5$ Å.

their phase shifts β_i and η_i defined in (2) and (3) can be obtained analytically through the energy-normalized base pair $f_i(R)$ and $g_i(R)$.

It the zero field case like the triatomic van der Waals molecular system of our interest here, on the other hand, analytical formulas for the elastic processes occurring in the region outside R_0 are not available. Besides, qdt parameters β_i and η_i for the elastic processes accrue their values from the same kind of the short-range potential as K matrices for the inelastic processes do. Therefore, locating the matching radius R_0 may be a more serious problem here than in the Coulombic system. [The motion of the van der Waals system is mostly dominated by an atom-additive Morse potential (17), hardly being affected by a long-range van der Waals interaction V_{vdW}. Accordingly, quantum defect parameters β_i and η_i accrue most of their values in the range of small radius because of the short-range nature of the potential (17).] It is thus quite possible that more energy sensitive phenomena taking place in the range of R, where the kinetic energy of the relative motion has a comparable size to the energy of the system, may already start from the small value of R at which channel couplings may no longer be ignored. If this is the case, the K matrix that incorporates the channel coupling effects may show a rather strong energy dependence. Thus, it is imperative to test carefully in the zero field case one of the fundamental tenet of MQDT that the real symmetric K matrix, eigenquantum defects μ_α and the frame transformation U matrix be slowly varying function of energy at the radius where the convergence of their values obtains. In subsections A through D, such an assumption will be tested.

Energy dependence of U matrices and μ_α. In Figure 2, a comparison of energy variations among μ_α is made for different values of $R_0=4$ Å, 4.5 Å and 5 Å. The reference potentials are the ones connected to the adiabatic potentials (will be simply called adiabatic reference potentials if no confusion arises). The connection parameters $R^*=3.75$ Å and $\rho=50$ are used for the reference potentials and calculations are performed with 6 channels, $\{v=0$ and $j=0, 2, 4\}$ and $\{v=1$ and $j=0, 2, 4\}$. At $R_0=4$ Å, the short range quantum-defects μ_α *vs.* energy are almost straight lines with small slopes. As the matching radius R_0 becomes larger, three among six curves in Figure 2 remain unaltered while the other three undergo changes in the shapes and magnitudes. Evidently, the former unaltering curves have mostly open channel contents. Larger R_0 bring about more avoided crossings. Convergence in μ_α obtains at $R_0\approx7$ Å. Figure 2 shows that no avoided curve crossings are observed for $R_0=4$ Å, one avoided crossing at $E\approx0.014$ eV for $R_0=4.5$ Å, and four at $E\approx0.01325$, 0.0142, 0.01475, and 0.0150 eV for $R_0=5$ Å. For $R_0=4.5$ Å and 5 Å, Figure 3 shows the great changes in the U matrix elements as functions of energy around the avoided curve crossings. [Here it is not utilized that only $N(N-1)/2$ among N^2 elements of the real U matrix (N denotes the number of channels) are independent because of the unitary relation among them. Instead, all N^2 matrix elements are plotted for brevity at the cost of the overlapped display of information. For two channel case, however, its utilization does not pose any difficulty and a single parameter, the mixing angle, is usually plotted in place of 4 matrix elements.]

Also Figure 2 shows the curve crossing besides avoided

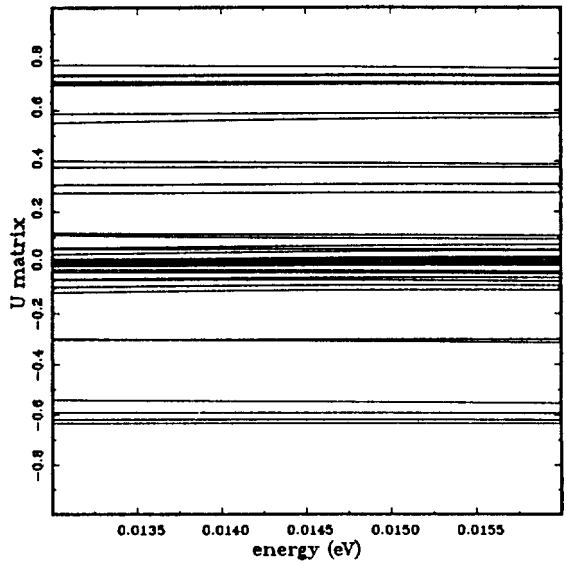

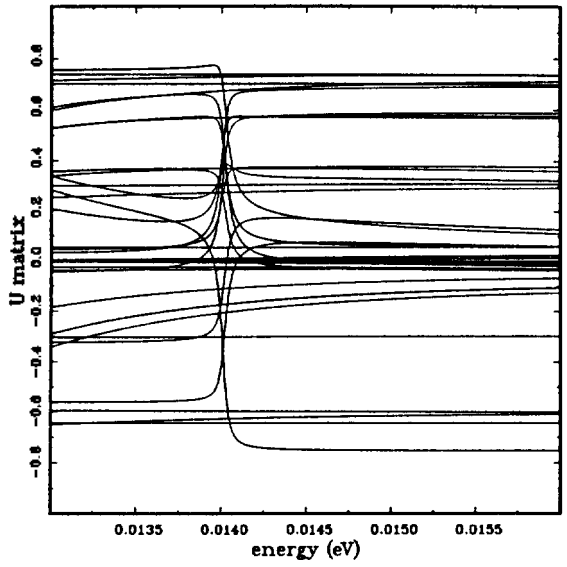

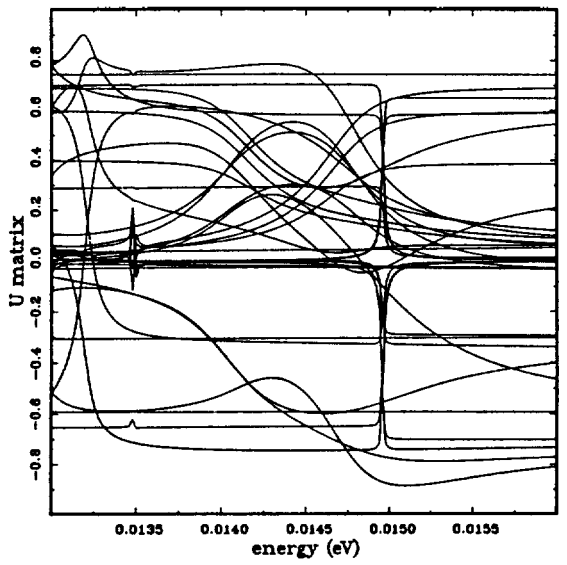

Figure 3. U matrix elements *vs* energy in the 6 channel calculation with (a) R_0=4 Å, (b) R_0=4.5 Å, (c) R_0=5 Å.

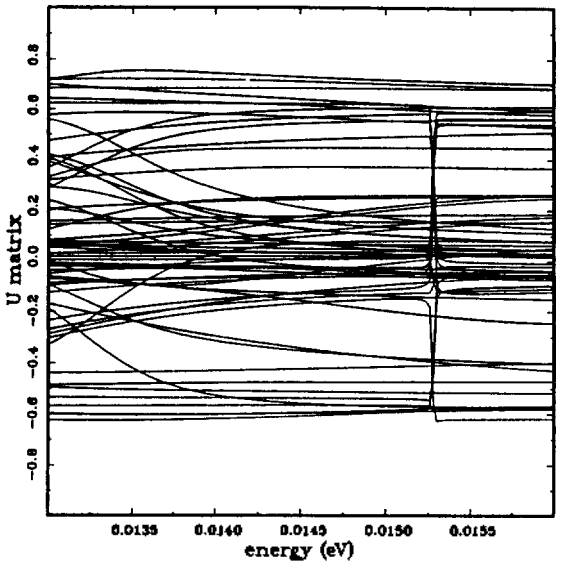

Figure 4. U matrix *vs* energy in the 8 channel calculation with R_0=4.5 Å.

curve crossings, *e.g.*, at $E\approx0.013$ eV for R_0=5 Å. Only a slight changes in U matrix elements are observed at the crossing points in Figure 3 in great contrast to the big changes around avoided curve crossings. While avoided crossings accompany changes in the nature of the short range channel wavefunctions, curve crossings without avoidance are not seen to lead to significant consequences.

For the reference potentials connected to the diabatic potentials, the short range quantum defect parameters μ_α converge slowly to the limiting values. The limiting values are common to both adiabatic and diabatic ones. They approach to the limiting values slowly up to $R_0\approx5$ Å, fast at 5 Å$\leq R_0\leq$6 Å and then converge to limiting values. Eigenquantum defects μ_α and $U_{i\alpha}$ vary as functions of energy slightly slower for these diabatic potentials than those for the adiabatic ones. As far as their values at small R_0 deviate from their limiting values more than those for the adiabatic reference potentials, and as far as the small R_0 are important regions for MQDT calculations as $U_{i\alpha}$ vary slowly there, there may be no point to consider the diabatic reference potentials. However, it practically yields better results than the adiabatic one. This point will again be considered in the later section.

If more channels are included into the calculations, stronger dependence of μ_α and $U_{i\alpha}$ on energy results in. In Figure 4, the effect of the number of channels is considered. U matrix elements at R_0=4.5 Å for 8 channel case show stronger energy dependence than for the 6 channel case. One more avoided curve crossing is observed for the former than the latter. For the van der Waals system, stronger energy sensitivity of μ_α and $U_{i\alpha}$ to the number of channels may be expected since the potential minima of the pure adiabatic or diabatic potentials become quickly higher as seen in Figure 1.

Energy dependence of β_i and η_i. QDT parameters β_i and η_i are shown in Figure 5 for the 8 channel case. They are smoothly varying functions of energy. Figure 5 shows that the rate of variation of β_i on energy is slower than the Coulombic ones, $\beta_i=\pi(\mu_i-1)$.

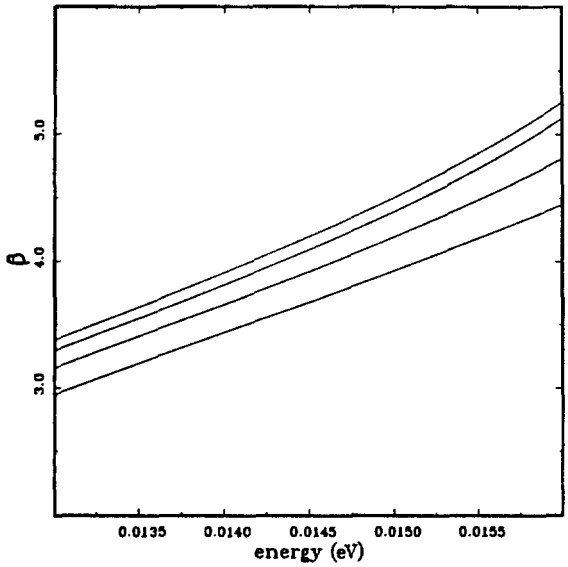

Figure 5. Quantum defect parameters β_i *vs* energy in the 8 channel calculation.

Consideration on the basic tenet of MQDT. The previous subsection IV. A shows the break-down of one of the fundamental assumptions of MQDT. Short-range qdt parameters μ_α and $U_{i\alpha}$ are found to be no longer slowly varying functions of energy at the radii of convergence of qdt parameters. The radius R_0 for the convergence of μ_α and $U_{i\alpha}$ is about 8 Å for the diabatic reference potentials and smaller for the adiabatic ones. The rapid variation of $U_{i\alpha}$ on energy is observed in that radius. The energy variation is much slower for μ_α than for $U_{i\alpha}$ at this range of R. [Recall, however, that the rapid variation observed at the frame transformation matrix U as a function of energy is caused by the avoided curve crossings in the eigenquantum defects μ_α. This implies that the energy variation of K matrix itself is somewhat similar to or slower than that of μ_α. The difference is in that curves are simply crossing in the K matrix while avoided in μ_α (the channel interactions bring about the avoided curve crossings in μ_α and the rapid variations in $U_{i\alpha}$ at the curve crossing points in the matrix elements of K). Thus at the radius of convergence, the K matrix itself remains as a slowly varying function of energy].

It may not be wanted that the nature of the short-range channel basis functions undergoes several drastic changes as exhibited in the energy variation of U matrix elements at the radius of convergence. Such a rapid variation of the U matrix as a function of energy does not necessarily reflect the change in the short-range frame wavefunctions as it enters at the region of R, 5 Å$\leq R \leq$7 Å. Rather, it reflects the fact that energy sensitive dynamics occurring at 5 Å$\leq R \leq$7 Å may affect the energy variation of U matrix much more here than in the Coulombic system as they begin to be included inside R_0 more and more. This implies that the MQDT framework described in Section II has to be reluctantly applied at R_0 smaller than the radius of convergence, where the R-dependence of the K matrix can not be ignored. If the R_0 dependence of the K matrix can somehow be incorporated into the framework of MQDT, more flexibility in choosing R_0 may result in and R_0 could be chosen as small as possible in order to drastically reduce the variation of U as a function of energy.

Calogero[25] long ago showed that K matrices satisfy Riccatti-type first-order nonlinear differential equations, alternative but equivalent to the close-coupling equation (similar work has appeared independently in different applications).[26] Note that the way by which the K matrix is obtained makes use of the same restrictions imposed in the Calogero method. In the K matrix calculation, arbitrary boundary conditions are imposed at the starting radius and solutions are propagated along R with the De Vogelaere algorithm. Then true wavefunctions are obtained by correcting this arbitrariness by imposing the restrictions (1) and

$$\frac{d\Psi_{i'}(R,\omega)}{dR} = \sum_i \Phi_i(\omega)\left[\frac{df_i(R)}{dR}\,\delta_{ii'} - \frac{dg_i(R)}{dR}\,K_{ii'}(R)\right] \tag{37}$$

at $R=R_0$ with the allowance of R-dependence of the K matrix. This is the one of the several restrictions considered in the Calogero method. Further consideration on this point is beyond the scope of this paper.

In the next subsection, we present the simple calculation that ignores the R dependence of the K matrix and that solves Eq. (9) by inserting the values of μ_α and $U_{i\alpha}$ by taking R_0 smaller than the radius of convergence. This simple calculation may not be quite bad since the R-dependence of the K matrix is still far smaller than those of $f_i(R)$ and $g_i(R)$. As it turned out, a good agreement of this simple calculation with close-coupling results is obtained, indicating that such a R dependence may not be quite critical.

Comparison of MQDT and close coupling calculations. Here we will compare MQDT calculations with the close coupling ones. The eigenphase sum of the S matrix is real and shows the resonance structure as proved by Hazi[27] and thus may be conveniently used for the comparison purpose in place of the complex-valued $N\times N$ S matrix elements themselves. The eigenphase sum σ of the S matrix is defined as the halfsum of the phases of the eigenvalues of the S matrix

$$\sigma = \sum_{\alpha=1}^{N_o} \delta_\alpha \tag{38}$$

with δ_α defined by

$$S_{ii'} = \sum_{\alpha=1}^{N_o} V_{i\alpha} e^{2i\delta_\alpha} V_{\alpha i'}^{\dagger} \tag{39}$$

where $V_{i\alpha}$ is the unitary matrix made of the eigenvectors of the S matrix and N_o is the number of open channels. The S matrix is here defined for the wavefunctions that satisfy the incoming wave boundary conditions *i.e.*

$$\Psi^{-(i')}(R,\omega) = \sum_i \Phi_i(\omega)[e^{ik_iR}\delta_{ii'} - e^{-ik_iR}S_{ii'}] \tag{40}$$

The wavefunctions $\Psi^{-(i')}(R,\omega)$ are obtained as a superposition of Ψ_ρ in MQDT, as considered in Eq. (14) with coefficients given by (15). Then the S matrix in the MQDT can be calculated from the formula

$$S_{ii'} = -e^{-i\eta_i}\sum_\rho T_{i\rho} e^{-2i\pi\tau_\rho} T_{\rho i'}^{-1} e^{-i\eta_{i'}} \tag{41}$$

(S matrices may be defined so that its eigenphase is given by $2\pi\tau_\rho$ instead of $-2\pi\tau_\rho$. This point has not been pursued further here as such a sign difference has no physical signifi-

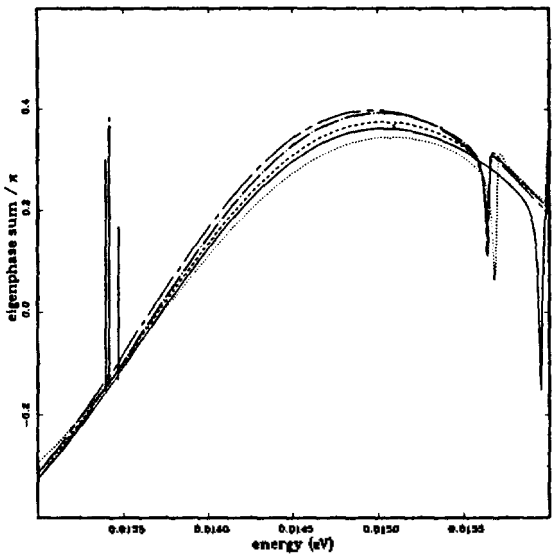

Figure 6. The comparison of eigenphase sums *vs* energy calculated by MQDT and close-coupling method for 6 channels: —, MQDT with R_0=4 Å; ···, MQDT with R_0=4.5 Å; ---, MQDT with R_0=5 Å; — · —, MQDT with R_0=6 Å; — - —, close coupling.

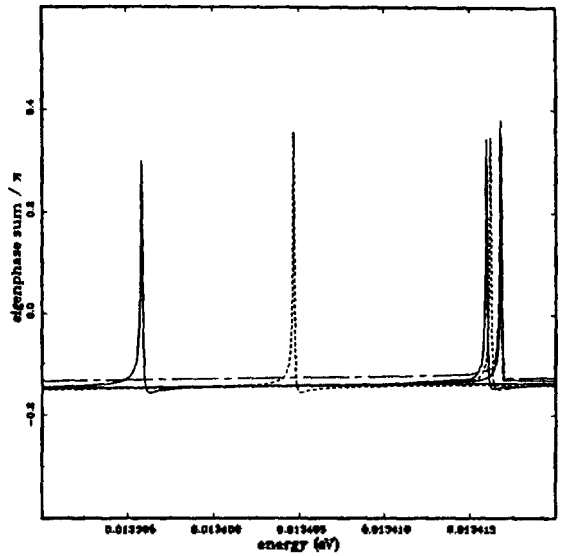

Figure 7. The comparison of eigenphase sums *vs* energy calculated from MQDT with close-coupling calculations for 6 channels in the vicinity of the first resonance. Solid and dashed lines denote MQDT calculations with adiabatic and diabatic reference potentials respectively. The peaks from the left correspond to R_0=4, 4.5, 5, and 6 Å calculations for each adiabatic or diabatic potentials respectively. MQDT calculation for R_0=6 Å is almost identical with the close-coupling one.

cance.)

Figure 6 compares the eigenphase sums (divided by π) obtained from 6 channel MQDT calculation with that of the close coupling one. V_{IOS} is here connected to the adiabatic potentials with R^*=3.75 Å and ρ=50. Quite remarkably, the background spectrum is already obtained at R_0=4 Å, namely, around the minima of the reference potentials. The first and second resonances located at $E\approx$0.013417 eV and 0.0156 eV are found at the shifted positions of 0.0135 and 0.0158 eV respectively, though. However, it is quite remarkable that such amounts of agreements obtain with only 2 energy mesh point calculation. With larger R_0=4.5 Å, we get better agreement on the resonance positions. The calculation can still be done with only a few mesh points if the energy is not close to the avoided curve crossing points. But even at the vicinity of avoided curve crossing points, we can do a very coarse mesh-point calculation. It is found that more coarse mesh-point calculations are possible with diabatic reference potentials. Even better agreements with close-coupling results can be anticipated and are obtained with larger R_0. More energy mesh points are, however, required for larger R_0, though the number of points still remains quite small in comparison with the close-coupling calculations.

Figure 6 also shows that the spectrum at the higher energies is more sensitive to the choice of R_0. This implies that more and more contributions to the eigenphase sums come from larger values of R with increase of energy. This point can be further confirmed by comparing two MQDT calculations with the better connection parameter, (R^*, ρ)=(3.85 Å, 50), and the poorer one, (4 Å, 25). For the latter, the portion of V_{IOS} in the reference potentials still survive and become excessive at large R where the adiabatic potentials are quite good representations of the true potentials. This persistence of V_{IOS} at large R only affects the higher energy spectrum.

The close-up of the region around the first resonance position is shown in Figure 7. It again confirms the general trend

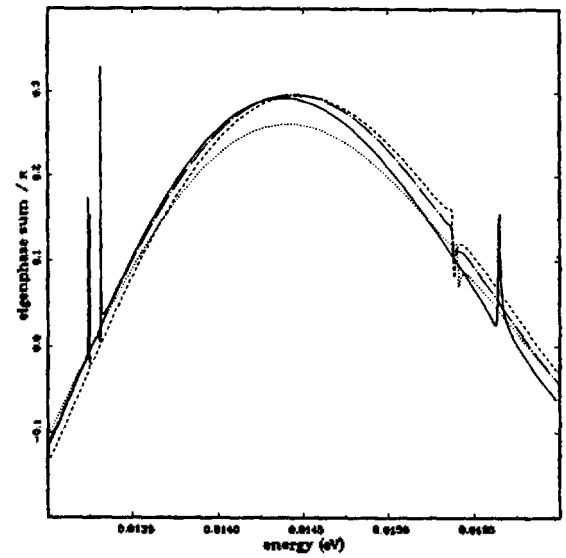

Figure 8. The comparison of eigenphase sums *vs* energy calculated from MQDT and close-coupling calculations with inclusion of 8 channels: —, MQDT with R_0=4 Å,···, MQDT with R_0=4.5 Å; — · —, MQDT with R_0=5 Å; ---, close coupling.

that larger matching radius R_0 yields better results. One of the interesting features of Figure 7 is that better results are obtained with diabatic reference potentials than with adiabatic ones. Note in Figure 7 that the resonance shapes are much more insensitive to R_0 and to the reference potentials than the resonance positions are.

Figure 8 shows the calculations with 8 channels that are almost enough number of channels to get the converged ei-

genphase sums. Reference potentials connected to the diabatic ones are used for the calculation of the base pair. Identical values of R^* and ρ are employed for the reference potentials in these calculations as in the 6 channel case. Again the agreement of MQDT calculations with close-coupling ones is excellent for larger R_0 and is good even for $R=4$ Å, though generally slightly poorer than the agreement in the 6 channel case. The discrepancies in the background spectrum and in the second resonance between two calculations are bigger here than the ones in the 6 channel calculations. This indicates that 8 channel calculations are more sensitive to the quality of reference potentials. Better agreement is expected to result in with the better reference potentials constructed with smaller R^* and larger ρ. This refinement is no further pursued in this work. Also, it is noted that the first resonance in the 8 channel calculation is of almost Lorentzian shape in contrast to the more asymmetric one in the 6 channel calculation.

Comparison between 6 and 8 channel calculations seems to suggest that the excellent result of the MQDT calculations with $R_0=4$ Å may not be an accidental one since the eigenphase sum undergoes a change more drastically with the change of channel numbers than with the change of R_0. This seems to imply that the decoupling of the close-coupling Eq. (23) already takes place at $R_0=4$ Å. This interpretation may not be quite absurd for the system of triatomic van der Waals predissociation since another very good approximation, IOS, for this system also assumes a decoupling in γ motion for all range of R. This point is further supported by the analysis in Section IV. A, as mentioned in Section IV. B.

The small R_0, such as 4 Å, calculation actually shows the complete disentanglement of the short-range from the long-range dynamics. The emergence of the strong energy dependence in the frame transformation U matrix at larger R_0 shows up the entrance of the long-range (though not quite long-range) strong energy dependence into the U matrix from the large R_0 region. The improvement is obtained only in the finest points with the inclusion of the range of large R into the K matrix in order to get the convergence of the K matrix. However, for the complete assessment of this phenomena, the theory of MQDT with the allowance of R_0-dependence into the K matrix should be developed further in the future. (The curve crossings that cause the rapid energy dependence may be lessened by making use of the analytic base pair f^0 and g^0).

Summary and discussion. Generalized MQDT formulated in Ref. 11 is implemented into the triatomic van der Waals predissociation process. In the implementation, we have tried from the outset to avoid specific assumptions usually practiced in numerous MQDT applications so that the method can be applied to any other systems by simply changing the potentials without touching the other part of the computer codes.

It turned out that the problem of choosing R_0 can not be ignored in the system of van der Waals predissociation system. This urges us to generalize MQDT further to allow the R_0-dependence of the K matrix.

Nevertheless, as a first approximation, we solved MQDT equation with neglect of the R_0-dependence of the K matrix. The agreement of MQDT and the close-coupling calculations is excellent, indicating that R_0-dependence of the K matrix may not be crucial. Also the study on the energy dependences of the short-range qdt parameters and of the frame transformation matrix on R_0 reveals that the complete separation of energy sensitive and insensitive contributions obtains at $R_0 \approx 4$ Å. More energy sensitive contributions enter at 4.5 Å$\leq R \leq$7 Å. In such an energy sensitive range, abrupt changes of the frame transformation matrix are detected around the avoided curve crossing points while eigenquantum defect curves μ are slowly avoiding each other. This observation shows one of the flexibility of MQDT calculation how we can avoid such an abrupt change in the frame transformation matrix by simply choosing R_0 smaller.

More energy sensitivity enters into MQDT calculations with more channels. In the potential parameters listed in Table 1, the convergence in the calculation is obtained with 8 channels. More channels will participate with the increase of the anisotropy and the reduced mass in the triatomic van der Waals system, narrowing the range of R_0 we can choose. However, the sensitivity of MQDT calculations to the number of channels observed in this paper seems to be the characteristics of the van der Waals predissociation system. Figure 1 shows how the minima of adiabatic or diabatic potentials move fast higher. For the H_2O system in its second absorption band, that occurs to a much less extent. Also, the systems used by Ref. 7 do not show such characteristis. This consideration indicates that experiences of the application of MQDT to more variety systems are called for in the future.

Acknowledgements. I would like thank Dr. R. Schinke for suggesting and supporting the research, and for many helpful discussions. I am indebted to Professor C. H. Greene for many helpful discussions and for carefully reading and editing the manuscript.

References

1. For the review, see M. J. Seaton, *Rep. Prog. Phys.*, **46**, 167 (1983).
2. U. Fano, *Phys. Rev.*, **A2**, 353 (1970); *J. Opt. Soc. Am.*, **65**, 979 (1975).
3. U. Fano and A. R. P. Rau, *Atomic Collisions* and *Spectra* (Academic, Orlando, 1986).
4. A. Giusti-Suzor and U. Fano, *J. Phys.*, **B17**, 4267 (1984).
5. C. H. Greene and Ch. Jungen, *Adv. At. Mol. Phys.*, **21**, 51 (1985).
6. (a) A. Giusti, *J. Phys.*, **B13**, 3867 (1980); (b) A. Giusti-Suzor and Ch. Jungen, *J. Chem. Phys.*, **80**, 986 (1984).
7. (b) F. H. Mies, *J. Chem. Phys.*, **80**, 2514 (1984); F. H. Mies and P. S. Julienne, *ibid*, **80**, 2526 (1984).
8. M. Raoult, *J. Chem. Phys.* **87**, 4736 (1987).
9. (a) K. C. Janda, *Adv. Chem. Phys.*, **20** 201 (1985); (b) J. I. Cline, N. Sivakumar, D. D. Evard, and K. C. Janda, *Phys. Rev.*, **A36**, 1944 (1987).
10. R. Schinke and J. M. Bowman, *Molecular Collision Dynamics* (Springer, Heidelberg, 1983) J. M. Bowman ed.
11. C. H. Greene, A. R. P. Rau, and U. Fano, *Phys. Rev.* **A26**, 2441 (1982).
12. L. I. Schiff, *Quantum Mechanics* (McGraw-Hill, New York, 1955).
13. A. R. P. Rau, *Phys. Rev.* **A4**, 207 (1971).
14. In order to understand that the form (3) corresponds

to the "energy normalized base pair" at negative energies, see Ref. 3, especially Chap. IV. A; see also Ref. 1, p. 187, for the explicit demonstration.
15. J. I. Cline, *et al., Structure and Dynamics of Weakly Bound Molecular Complexes* (D. Reidel, Dordrecht, 1987), A. Weber, ed.; J. C. Drobit and M. I. Lester, *J. Chem. Phys.*, **86**, 1662 (1987).
16. N. Halberstadt, J. A. Beswick, and K. C. Janda, *J. Chem. Phys.*, **87**, 3966 (1987).
17. M. S. Child, *Molecular Collision Theory* (Academic, London, 1974).
18. R. G. Gordon, *J. Chem. Phys.*, **51**, 14 (1969).
19. See, *e.g.*, J. L. Powell and B. Crasemann, *Quantum Mechanic* (Addison-Wesley, Palo Alto, 1961); for the exhaustive list of references, H. J. Korsch and H. Laurent, *J. Phys.* **B14**, 4213 (1981).
20. Byungduk Yoo and C. H. Greene, *Phys. Rev.*, **A34**, 1635 (1986).
21. W. Lester, Methods. *Comput. Phys.*, **10**, 243 (1971).
22. J. Dubau and M. J. Seaton, *J. Phys.*, **B17**, 215 (1984).
23. A. Giusti-Suzor and U. Fano, *J. Phys.*, **B17**, 215 (1984).
24. C. H. Greene, U. Fano, and G. Strinati, *Phys Rev.*, **A19**, 1485 (1979).
25. U. Fano, C. E. Theodosiou, and J. L. Dehmer, *Rev. Mod. Phys.*, **48**, 49 (1976); For the application of Calogero method to MQDT see C. H. Greene, *Phys. Rev.*, **A20**, 656 (1979).
26. See Ref. 18; F. H. Mies, *Mol. Phys.*, **41**, 973 (1980).
27. A. U. Hazi, *Phys. Rev.*, **A19**, 920 (1979).